Published in final edited form as:

Cell. 2015 October 8; 163(2): 394–405. doi:10.1016/j.cell.2015.09.021.

Formation of a neurosensory organ by epithelial cell slithering

Christin S. Kuo[1,2,3] and **Mark A. Krasnow**[1,3]

[1]Department of Biochemistry, Stanford University School of Medicine, Stanford CA, 94305-5307

[2]Department of Pediatrics, Stanford University School of Medicine, Stanford CA, 94305-5307

[3]Howard Hughes Medical Institute, Stanford University School of Medicine, Stanford CA, 94305-5307

Abstract

Epithelial cells are normally stably anchored, maintaining their relative positions and association with the basement membrane. Developmental rearrangements occur through cell intercalation, and cells can delaminate during epithelial-mesenchymal transitions and metastasis. We mapped the formation of lung neuroepithelial bodies (NEBs), innervated clusters of neuroendocrine/neurosensory cells within the bronchial epithelium, revealing a targeted mode of cell migration that we named “slithering,” in which cells transiently lose epithelial character but remain associated with the membrane while traversing neighboring epithelial cells to reach cluster sites. Immunostaining, lineage tracing, clonal analysis, and live imaging showed that NEB progenitors, initially distributed randomly, downregulate adhesion and polarity proteins, crawling over and between neighboring cells to converge at diametrically-opposed positions at bronchial branchpoints, where they reestablish epithelial structure, express neuroendocrine genes. There is little accompanying progenitor proliferation or apoptosis. Activation of the slithering program may explain why lung cancers arising from neuroendocrine cells are highly metastatic.

Graphical Abstract

Correspondence to: Dr. Mark Krasnow <krasnow@stanford.edu>, 650-723-7191 (phone), 650-723-6783 (fax).

Author contributions

C.S.K. and M.A.K. conceived project and designed experiments, C.S.K. executed and analyzed experiments and C.S.K. and M.A.K. and wrote the manuscript.

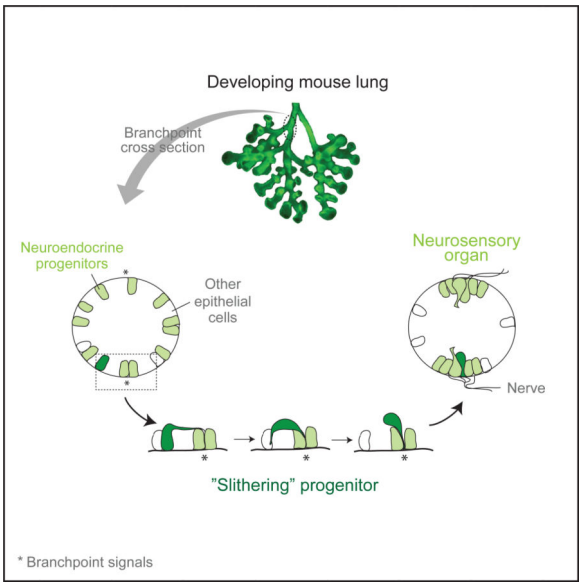

Introduction

Epithelia are sheets of cells that line and protect the body and internal organs, and the polarized cells that comprise them play important roles in absorption, secretion, and sensation. Epithelial cells are normally tightly attached to one another through specialized junctions and adhesion proteins along their lateral surface, and anchored to the basement membrane at their basal surface. Although epithelial sheets can grow and change shape, the constituent cells typically maintain their relative positions. When cells in an epithelial monolayer have been found to rearrange, as in *Drosophila* germ band elongation (Irvine and Wieschaus, 1994) and wing morphogenesis (Aigouy et al., 2010), they do so conservatively by cell intercalation, in which cells shrink lateral junctions with some neighboring cells while expanding lateral junctions with others, exchanging positions while maintaining their polarized structure and the integrity of the epithelium (Bertet et al., 2004; Blankenship et al., 2006; Guillot and Lecuit, 2013). Here we describe a very different mode of epithelial cell rearrangement that results in homotypic sorting (Krens and Heisenberg, 2011) of a specialized cell type, discovered in our dissection of pulmonary neuroendocrine (NE) cell development in mice.

Pulmonary NE cells are one of the most interesting but least understood cell types in the lung. They are distributed throughout the bronchial epithelium, interspersed among secretory club (Clara) cells and ciliated cells, the two major airway epithelial cell types (Rock and Hogan, 2011). Like other neuroendocrine cells in the body, they were originally identified by their secretory dense-core vesicles (Feyrter, 1954) that contain signaling molecules and bioactive peptides, including serotonin and calcitonin gene-related peptide (CGRP). Although some pulmonary NE cells are distributed randomly in the airway epithelium, others are organized into clusters called neuroendocrine or neuroepithelial bodies (NEBs) that are highly innervated (Brouns et al., 2008; Lauweryns and Peuskens, 1972), forming synaptic contacts with afferent and efferent nerve fibers (Lauweryns and

Van Lommel, 1987). NE cells can be activated by a variety of stimuli and are thought to monitor diverse aspects of lung physiology including oxygen, chemical, and mechanical changes (Cutz et al., 2013). In addition to these sensory and neurosecretory functions, NE cells have a stem cell function that helps replenish the bronchial epithelium following severe injury (Guha et al., 2012; Reynolds et al., 2000; Song et al., 2012). They are also the initiating cells of small cell lung cancer (Park et al., 2011; Song et al., 2012; Sutherland et al., 2011), a highly metastatic and the most deadly form of lung cancer (van Meerbeeck et al., 2011). Excess or altered distribution of NE cells are also found in a variety of serious but poorly understood lung diseases including sudden infant death syndrome (SIDS) (Cutz et al., 2007), bronchopulmonary dysplasia (BPD) (Gillan and Cutz, 1993), and neuroendocrine hyperplasia (Aguayo et al., 1992; Deterding et al., 2005).

To provide a foundation for a genetic dissection of the development, function, and diseases of pulmonary NE cells, we first mapped their locations in mice and found that NEBs are located at stereotyped positions. We then probed NEB development by immunostaining, lineage tracing, and imaging of developmental intermediates, and found that although progenitors are initially distributed randomly throughout the epithelium, they rapidly resolve into clusters. We show that clusters do not form by progenitor proliferation, but by a targeted mechanism of epithelial cell rearrangement in which progenitors transiently lose epithelial character as they “slither” over and around neighboring cells and converge at cluster sites.

Results

Mapping the origin and distribution of NEBs

Pulmonary NE cells are distributed sparsely throughout the bronchial epithelium both as solitary cells and clusters. Most mature NE cells are typical columnar epithelial cells, however some have distinct morphologies such as short “pyramidal” cells that do not reach the surface or slender cells with a thin luminal projection (Fig. 1A,B). Clusters are either small, typically with 2-5 NE cells, which we call “mini-clusters” (Fig. 1C), or are larger clusters typically containing 20-30 NE cells (Fig. 1D,E). The terms “neuroepithelial body” (NEB) and “neuroendocrine body” often refer to all NE cell clusters, but here we reserve the term NEB for large clusters. NE clusters in other species are innervated (Lauweryns and Peuskens, 1972; Scheuermann, 1987), and we found by immunostaining for neurites with PGP9.5 (Uchl1) that mouse NEBs are extensively innervated and mini-clusters show some innervation, whereas solitary NE cells do not appear to be innervated.

We mapped the locations of NE cells in the mouse bronchial tree in late stage embryonic lungs (embryonic day E16 - E18) using the airway branch lineage (Metzger et al., 2008). NE cells were detected by immunostaining for the proneural bHLH transcription factor Ascl1 (Mash1) or cytoplasmic NE marker PGP9.5, or using an *Ascl1*^{CreER} lineage trace, which within the bronchial epithelium labels exclusively the NE lineage (Fig. S1). We analyzed serial sections of left lung lobes co-stained for E-cadherin to visualize airway epithelium. Solitary NE cells and mini-clusters were scattered throughout the bronchial epithelium in no obvious pattern. The pattern of NEBs, however, was highly stereotyped. NEBs localized exclusively to airway branchpoints (Fig. 1F,G). Although none were found at the origin of

the trachea or right and left primary bronchi, at every branchpoint examined beyond this a pair of NEBs was present (Figs. 1F,G, and S2). NEBs were located at diametrically-opposite positions at branch junctions, with one at the most proximal position and the other the most distal (Fig. 1H,I). Hence, we designate each NEB by the name of the branch it originates, plus “p” or “d” to distinguish proximal and distal partners. The proximal NEB marks the most obtuse angle of the branch junction, whereas the distal NEB lies at the most acute angle. The same pattern was observed at every branchpoint examined in other lobes (Fig. S2) (n=5 lungs, 70 branchpoints). Thus, NEBs form at stereotyped, diametrically-opposite positions at secondary airway branchpoints and beyond, implying there is a localized signal directing NEB formation at each of these sites.

NE cells in other organs arise either from invading neural crest cells that colonize the organ or by differentiation of resident epithelial cells (Anderson and Axel, 1986; Gu et al., 2002). Initial lineage trace studies indicated that at least some pulmonary NE cells arise from the epithelium (Song et al., 2012). To determine if NEBs arise from the epithelium, we used a *Sonic hedgehog*^{Cre} (*Shh*^{Cre}) knock-in allele (Harris et al., 2006) and a Cre recombinase reporter to label and lineage trace developing airway epithelial progenitors several days before NE progenitors are detected. At E18.5, all NEBs as well as mini-clusters and solitary pulmonary NE cells expressed the *Shh*^{Cre} lineage trace (n=500 NE cells scored) (Fig. 1J,K). In a similar experiment using a *Wnt1-Cre* transgene to lineage trace developing neural crest cells, no NE cells at E18.5 expressed the lineage trace (n=500) (Fig. 1L). We conclude that all pulmonary NE cells, including NEBs, arise from the *Shh* epithelial lineage, not from neural crest. Thus, both solitary and clustered pulmonary NE cells share the same origin as other airway epithelial cells.

Three phases of NEB development

To elucidate the cellular events and timing of NEB formation, we mapped the development of specific NEBs beginning at E12, before NE progenitors are detected, through E16 when NEBs achieve their characteristic structure. We used Ascl1, the earliest known marker of NE cells (Ito et al., 2000), to visualize progenitors and early events, and PGP9.5 and CGRP, canonical markers of mature NE cells (Polak et al., 1993), to visualize later steps. We analyzed five serially-sectioned wild-type CD-1 lungs at each of six stages between E12-E16, initially focusing on the base of branch L.L2 where NEBs L.L2p and L.L2d form (Fig. 2). The earliest NE progenitors at these sites were detected at late E12.5 to E13, when a few scattered cells in the epithelium began to express Ascl1 (Fig. 2A). At E13, more densely distributed but still solitary NE progenitors were present in a “salt and pepper” pattern (Fig. 2B). By late E13.5 to E14, small groups of NE progenitors were detected at L.L2p and L.L2d and also scattered around the region (Fig. 2C). By E14.5, within 24-48 hours of detection of the first NE progenitors, numerous small clusters of NE cells began to appear throughout the region, interspersed with solitary cells (Fig 2D, S3B). At E15.5, large clusters of NE cells were detected, but exclusively at the positions of NEBs L.L2p and L.L2d (Fig. 2E). By E15.5 – E16, NE cells in NEBs L.L2p and L.L2d expressed PGP9.5 and CGRP, as did solitary NE cells and mini-clusters in the region (Figs. 2F, S3E,F). This analysis subdivided NEB formation into three developmental phases: NE cell selection (E12.5 to E13.5), cluster formation (E13.5 to E15.5), and differentiation (E15.5 onward).

During differentiation, PGP9.5-positive nerve fibers extend toward and begin to ramify on the NEB (Fig. 2F; Fig. S3G-I).

The same series of cellular events and developmental phases was observed at other positions where NEB formation was mapped, including L.L3p/L.L3d, L.L4p/L.L4d, and L.L5p/L.L5d, all located at the base of secondary branches along the left primary bronchus. However, the process initiates slightly later at the more distal positions, delayed by about 0.5 day for L.L3, 1 day for L.L4, and 1.5 days for L.L5 NEBs. This is best appreciated in images capturing all four positions in the same lung, when the most distal branch (L.L5) has not yet initiated NE development, L.L4 is undergoing NE cell selection, L.L3 has begun NE clustering, and L.L2 is in the NE differentiation phase (Fig. S3A,B). Thus, NEBs form in three phases - NE selection, cluster formation, and differentiation - that initiate in a proximal-to-distal sequence separated by about a half day between branches along the left primary bronchus. Despite differences in the timing of NEB program initiation along the proximal-distal axis, the differentiation phase begins in near synchrony for all NEBs and other NE cells (Fig. S3G-I), suggesting that this final phase is triggered by a more global signal independent of earlier steps in the program.

Cluster formation does not occur by proliferation of NE precursors

NE and neurosensory cells in many tissues are arranged in clusters, but how clusters form is only understood for Drosophila and other insect sensory bristles. Each Drosophila bristle arises by proliferation of a single progenitor expressing Achaete-Scute proteins (founders of the *Ascl1* gene family), and the clonal cell cluster differentiates into bristle sensory and support cells (Cubas et al., 1991; Lawrence, 1966). To determine if NEBs form by clonal proliferation of an epithelial progenitor, we labeled all airway epithelial progenitors prior to NEB formation using Shh^{Cre} and the "Rainbow" ($Rosa26^{Rbw}$) Cre-reporter (Rinkevich et al., 2011), which stochastically and permanently labels each progenitor and any of its daughter cells with one of three different fluorescent proteins. If NEBs form like Drosophila sensory bristles, each mature NEB should be monoclonal and hence composed of cells of a single Rainbow color. We found instead that all NEBs examined at E17.5-E18 (n>100), including those examined closely by confocal microscopy to distinguish individual NE cells, were multi-colored (Fig. 3A; Table S1). A similar result obtained for NE miniclusters. Thus, NEBs and miniclusters arise from multiple founder cells, not clonal proliferation of a single NE progenitor.

Although the above results rule out NEB formation by proliferation of a single progenitor, they do not exclude the possibility that NEBs are polyclonal, arising by proliferation of multiple NE progenitors. We therefore carried out two types of experiments to investigate the role of progenitor proliferation in NEB formation. We first used an inducible Cre recombinase (Cre-ER) expressed from the endogenous *Ascl1* promoter ($Ascl1^{CreER}$) (Kim et al., 2011), and an early (~E11.5-E12) dose of the inducer tamoxifen, to sparsely label individual NE progenitors with one of the Rainbow colors. When mature NEBs and miniclusters were examined 6 days later, few clusters were labeled, and of those that were most contained just a single labeled cell (30 of 39 labeled clusters) (Fig. 3B). In those with more than one labeled cell, the cells were usually different colors, in the ratio expected for

independent labeling events (Table S2). This implies that there is little or no proliferation of NE progenitors once they express the progenitor marker Ascl1. A similar conclusion obtained by pulse-labeling with deoxyribonucleotide analogue EdU from E12-E15 to detect dividing NE cells. Although EdU-labeled cells were readily detected in surrounding (non-neuroendocrine) epithelial cells and mesenchyme, few labeled NE cells were detected (Fig. 3C,D). The only labeled NE cells (<1% of NE cells) were solitary NE progenitors in the most distal regions of the bronchial tree just initiating *Ascl1* expression. We conclude that NE progenitors cease dividing at or shortly after initiation of *Ascl1* expression, and proliferation of progenitors does not contribute significantly to cluster formation.

Local clearing of NE cell precursors without apoptosis

Inspection of the airway epithelium immediately surrounding positions where NEBs form showed local “clearing” of NE progenitors: progenitors were initially evenly distributed in a salt and pepper pattern like other regions, but labeled cells were lost as NEBs formed nearby (Fig. 4A). To determine if clearing was due to programmed cell death, we examined the regions for expression of the apoptosis marker activated Caspase-3. Although activated Caspase-3 was detected in other developing cell types, little or none was detected in Ascl1-expressing NE progenitors (Fig. 4B,C). Cell counts also showed no decline in NE progenitors during cluster formation (Fig. S3C,D). Thus, apoptosis does not contribute to clearing of NE progenitors from regions surrounding NEB formation.

Sparse labeling reveals a series of migratory NE intermediates

Local clearing of progenitors and declining number of solitary NE cells as the number of clustered cells and size of the clusters increased (Fig. S3C,D) suggested that NEB formation might occur by local sorting of NE progenitors. To identify and visualize developmental intermediates, we sparsely labeled NE progenitors at E11.5 or E12.5 using $Ascl1^{CreER}$ and limiting tamoxifen in conjunction with the $Rosa26^{ZsGreen}$ reporter that robustly labels NE progenitors, allowing visualization of the full structure of individual intermediates (Figs. S5,and S6). Examination of labeled progenitors 2 - 4 days later revealed a collection of developmental intermediates with striking migratory morphologies (Fig. 5A), including long cytoplasmic extensions, fibroblast-like shapes oriented orthogonal to neighboring epithelial cells - some fully detached from the basement membrane - and cells spiraling around each other and converging at the basement membrane (Fig. 5B-F). NE cells with migratory structures were abundant in regions surrounding sites of NEB formation, and they were transient intermediates detected only during NEB formation (labeling between E12 and E13 but not at E14 or later) that “chased” into mature NEBs in the 36 hours after labeling. The migratory morphologies were specific to the NE lineage as other epithelial cells labeled during this period using $FoxA2^{CreER}$ showed the typical structure of monolayer or pseudostratified epithelial cells (Fig. S4).

Analysis of over 180 labeled NE intermediates (Table S3) by confocal microscopy distinguished five morphologic classes. Class 1 cells were the earliest and simplest intermediates: solitary NE cell progenitors lacking extensions or unusual morphologic features (Fig. 5B). They are early progenitors, presumably before migration has occurred, as they were the only labeled cells detected during the earliest pulse-chase interval (E11.5-

E13.5). Class 5 intermediates were similar in structure to Class 1 cells, each showing normal epithelial structure and orientation, except Class 5 cells were found in clusters (Fig. 5F). Class 5 cells are the most advanced intermediates because they were the only type detected at E16.5 and later (Fig. 5G). The other three classes had migratory morphologies, and were the most striking and unusual structures. Class 2 intermediates are solitary and resemble Class 1 intermediates with a largely normal epithelial morphology, except they have a long (up to 30 μm) cellular extension that reaches over or around neighboring epithelial cells, typically contacting another NE cell several cell diameters away (Fig. 5C, Table S3). Class 3 intermediates have the most surprising structure, betraying their epithelial origin. They resembled fibroblasts and had protrusions and often twisted morphologies that curved over or around, and occasionally under neighboring epithelial cells. Some had no detectable contact with the basement membrane, or contacted it only via a thin cellular extension (Fig. 5D). Class 4 intermediates were associated with other NE cells, organized into nascent clusters with cell bodies localized apically and thin extensions swirling as they converged at a site on the basement membrane (Fig. 5E).

We inferred from the structures of the intermediates that they comprise a developmental series, beginning with Class 1 and proceeding sequentially to Class 5 (Fig. 7A): NE progenitors first extend long processes and move toward their target at a branch junction, losing their epithelial structure and adopting a mesenchymal morphology as they leave their birth site. They then migrate to the target, converging there with other progenitors and re-establishing their epithelial structure and organizing into clusters. Similar intermediates were observed at sites of mini-cluster formation (Table S3), suggesting that miniclusters form by a related sorting process.

The timing and location of intermediates at sites of NEB formation support the proposed sequence. Quantification of the abundance of each type of intermediate at the same site (along the primary left lobe bronchus) but different times in NEB development (E13.5 - E16.5; Fig. 5G), or at different stages in the developmental process (represented by different positions along the proximal-distal axis (L.L4, L.L3, L.L2) at the same time in development (E14) (Fig. 5H-K), supported the proposed order. Class 5 intermediates were also the only ones innervated, confirming they are the most mature. Marker expression patterns provide further support for the proposed sequence, with expression of progenitor marker Ascl1 present in Class 1 and 2 but progressively declining in Class 3, 4, and 5 cells, and expression of late NE markers initiating in Class 4 (PGP9.5) and 5 (CGRP) cells (Fig. 2; Fig. 7A, B).

Live imaging of NE migration during cluster formation

To investigate dynamics of progenitor migration and sorting, we developed a slice culture preparation from transgenic *Ascl1*$^{CreER/+}$;*Rosa26*$^{ZsGreen/mTmG}$ embryonic mouse lungs with NE progenitors labeled with ZsGreen and membrane GFP (mGFP), and other cells labeled with mTomato. This allowed tracking by time-lapse confocal microscopy of individual NE progenitors for 2-3 days in the 175 μm thick lung slices as they moved toward and integrated into target sites. This showed progenitors migrating toward targets at 1 - 3 μm per hour, dynamically extending processes and changing shape as they crawled over and around neighboring epithelial cells (Fig. 6A-M; Movie S1). Progenitors migrated tens of microns or

more, traversing many neighboring epithelial cells or even crossing from one side of a developing bronchial tube to the other when the sides were apposed (Figure 6N-V; Movie S2). Periodically, the migrating cells paused ("resting", Fig. 6I,M, Movie S1) or changed direction (Fig. 6J, "extending away"; Movie S1), or displayed dynamic interactions with other NE cells ("kissing", Fig. 6F-H, Movie S1) or the basement membrane ("dynamic anchors", Fig. 6R,S, Movie S2). After the progenitor approached the target, this slow and halting migration phase was followed by direct and rapid (~5 μm/hr for 2 hr) entry into the developing cluster. Live imaging confirmed this mode of NE cell migration predicted by the in vivo intermediates, and it revealed dynamic "exploratory" behaviors and interactions with other NE cells and the basement membrane as migrating cells seek and ultimately converge at the target.

Transient down-regulation of epithelial adhesion and polarity in migrating progenitors

The intermediates and movements imply that NE progenitors undergo changes in adhesion and polarity as they migrate and form a NEB. To begin to elucidate the underlying molecular events, we immunostained intermediates for adhesion and polarity markers (Fig. 7A,C-E). E-cadherin showed dynamic changes in expression during cluster formation (Fig. 7 A,C). The adhesion protein was expressed at normal levels in early progenitors but dramatically down-regulated in migrating Class 3 intermediates. Down-regulation was transient because E-cadherin was again detected in Class 5 intermediates that reached their target and re-established full contact with the basal lamina, although even then E-cadherin levels remained below that of surrounding non-NE epithelial cells. Immunostaining also showed induction of neural cell adhesion molecule (NCAM) during NEB formation. NCAM was expressed in Class 5 intermediates (Fig. 7A, S7B), implying a role in NEB assembly or cohesion.

Immunostaining for epithelial apicobasal polarity markers β1, laminin γ1, and zona occludens-1 (ZO-1), and analysis of the apicobasal distribution of E-cadherin, showed that developing NE cells also undergo dynamic changes in polarity. Progenitors prior to NE cell selection (Figs. 7D, S7A), and epithelial cells not selected (Fig. S7C,D), show the expected apicobasal distribution of markers (Fig. 7A). However, early NE progenitors (Class 1 and 2) lose integrin β1 and ZO-1 expression, and E-cadherin is distributed around the entire plasma membrane; the only apparent residual polarity is contact with the laminin γ1-expressing basal lamina (Figs. 7A). Migrating Class 3 intermediates appear to have lost epithelial structure and polarity, with E-cadherin expression diminished as noted above and no contact with the basal lamina or only residual contact in local areas of low or undetectable laminin γ1 (Fig. 7C,D and S7A). Class 4 intermediates begin to reestablish epithelial structure with E-cadherin again detected surrounding the entire cell, and their thin cytoplasmic extensions converging and contacting laminin in the basal lamina, suggesting re-initiation of apicobasal polarity (Fig. 7A,D). Class 5 intermediates show continued maturation of epithelial structure and polarity that is complete in at least some cells, as evidenced by an expanded site of contact with laminin and basal lamina, expression of integrin β1 (Fig. S7A) along the entire basolateral surface, and expression of ZO-1 at the apical plasma membrane and exclusion of E-cadherin from this domain (Figure 7A,D).

These morphological and molecular changes show that NE progenitors undergo a transient epithelial-to-mesenchymal transition (EMT) during migration and NEB formation. Many EMT events are controlled by Snail proteins, zinc finger transcription factors that drive the switch (Mani et al., 2008; Strobl-Mazzulla and Bronner, 2012). Using anti-Snail antiserum to detect Snail 1, 2 and 3, none was detected in the earliest NE progenitors or any other epithelial cells (Fig. 7A,E). However, soon after initiation of Ascl1 expression, nuclear Snail was detected and expression continued throughout cluster formation, before declining in Class 5 intermediates as NE clusters form and re-establish epithelial structure and Ascl1 levels decline. We conclude that early NE progenitors induce Snail expression and undergo EMT, although it is an unconventional EMT as progenitors remain associated with the epithelium and the process soon reverses as progenitors downregulate Snail and restore epithelial structure and polarity on reaching the target.

Discussion

We have shown that NEBs form from NE progenitors initially distributed apparently randomly in the bronchial epithelium but then resolve in two days into clusters of 20-30 NE cells at stereotyped, diametrically-opposed positions at the base of each bronchial branch. There is little or no progenitor proliferation during the process, so NEBs do not form by clonal expansion, as do Drosophila and other insect neurosensory organs. There is also little if any apoptosis of progenitors or reduction in progenitor number, so the clearing of progenitors from regions surrounding developing NEBs is not due to programmed cell death. Instead, lineage tracing, sparse labeling of progenitors, and high resolution imaging of intermediates in vivo, together with live imaging of progenitors in lung slices ex vivo, show that progenitors lose epithelial character and adopt fibroblast-like morphologies as they slowly (1-3 μm/hour for 1-2 days) crawl over and around neighboring epithelial cells, converging at diametrically opposed sites at the base of each bronchial branch, and then rapidly (1-2 hours) joining the cluster. The intermediates express EMT transcription factor Snail and transiently down-regulate E-cadherin and epithelial polarity proteins, and then re-express these adhesion and polarity proteins and turn on NE differentiation genes and NCAM as they re-establish epithelial structure and assemble into a neurosensory organ.

The results lead us to propose that NEBs form by a targeted mode of epithelial cell sorting we call “slithering,” in which the rearranging cells transiently lose epithelial structure and polarity yet remain intimately associated with the epithelial sheet as they traverse neighboring epithelial cells and converge at the target site. This mechanism of cell rearrangement differs dramatically from intercalation, the classical mode of epithelial cell rearrangement, in which cells shrink lateral junctions with some neighboring cells while expanding junctions with others, exchanging positions while maintaining their polarized structure (Bertet et al., 2004; Blankenship et al., 2006; Guillot and Lecuit, 2013). At a mechanistic level, slithering is more reminiscent of cell delamination by EMT (Lamouille et al., 2014), such as during cancer metastasis (Scheel and Weinberg, 2012) or in neural crest formation where neural tube cells detach from the basement membrane and become mesenchyme-like cells that colonize distant sites (Strobl-Mazzulla and Bronner, 2012). During slithering, however, NE precursors never (or only transiently) leave the epithelial layer and they move comparatively short distances (10's of microns), and then rapidly regain

epithelial character, so it is only a fleeting conversion. Epithelial cells can also undergo partial EMT during branching morphogenesis, in some organs forming highly dynamic, proliferative cell clusters at bud tips (Ewald et al., 2008), and individual proliferating epithelial cells can even occasionally send daughter cells to non-adjacent positions in the monolayer ("mitosis-associated cell dispersal") (Packard et al., 2013). However, unlike these apparently random epithelial cell rearrangements and dispersals, slithering occurs without proliferation and is selective, directed, and purposeful. It results in active sorting of NE cells from surrounding epithelial cells in the monolayer, contrasting with the passive mechanisms long envisioned for cell sorting (Krens and Heisenberg, 2011; Steinberg, 1963) and forming neurosensory organs at defined positions.

Two prominent features of slithering are its selectivity for NE cells and their specific targeting to diametrically-opposed positions at the base of each bronchial branch, raising the questions: what provides the guidance cue and its selectivity for NE cells? Because of the dynamic exploratory behavior of NE cells during slithering, we favor the idea that the guidance cue is a chemoattractant. And, because only NE cells slither and they do so after turning on the master transcription factor Ascl1, we suggest that the chemoattractant receptor is specific for NE cells and part of their developmental program. However, there is no obvious cell or structure at target sites that could provide a point source of chemoattractant, and neurites that innervate NEBs arrive at their target only after the clusters form (Figs. 2F, S3G-I). Perhaps the cue is a combination of more broadly distributed but overlapping signals, or even a physical signal related to the target structure: NEBs form at the most proximal and distal positions of the branch junction, where the connecting branches form the most obtuse (proximal) and acute (distal) angles. Although we have not systematically studied the formation of mini-clusters, available data indicate that they, too, form by slithering. However, because they do not form at stereotyped positions, their clustering could be driven by a homotypic attraction signal. A homotypic signal may also contribute to NEB formation, as real time imaging showed repeated transient contacts ("cell kisses") among progenitors entering a NEB. A high priority now is to identify the signal(s) and their sources and receptors that control slithering, and to determine if the same signals also guide outgrowth of neurites that target NEBs.

Because of the similarity in their developmental origins and clustered structures, slithering may also be used to form other epithelial neurosensory organs such as taste buds (Chai et al., 2000; Okubo et al., 2009) and Merkel touch domes in skin that mediate light touch and spatial discrimination (Morrison et al., 2009; Van Keymeulen et al., 2009; Wright et al., 2015). And, because slithering is difficult to detect without membrane marking or live imaging of individual intermediates, slithering could be a more widely used mechanism of movement and sorting of epithelial cells that has been overlooked even in well-studied epithelia such as the intestinal crypt, where Paneth cells move down from the proliferative zone as other cells move up (Batlle et al., 2002). Slithering appears to be a late evolutionary innovation, at least in the lung, because although all mammals studied have NEBs, the most primitive extant fish species have only solitary pulmonary NE cells (Zaccone et al., 1989).

It will be important to identify the slithering program and indeed the full program of NEB formation including cell selection, migration, differentiation, and innervation, and how these

processes go awry in Notch pathway mutants (Morimoto et al., 2012; Tsao et al., 2009) and other forms of pulmonary NE cell disease including those with excess or misplaced NE cells (Nassar et al., 2011; Young et al., 2011). One appealing idea is that the slithering program is transiently reactivated in their stem cell function as they move out of their niche to replace dying neighboring cells, and permanently activated by mutation during oncogenesis. The latter could explain why small cell lung cancer arising from pulmonary NE cells metastasize early and are the most deadly form of lung cancer.

Experimental Procedures

Animals

CD-1 was wild type strain. Cre alleles and reporters are described in Supplemental Experimental Procedures.

Immunohistochemistry and histology

Embryos and lungs from timed pregnancies, with noon of the day of vaginal plug detection designated E0.5, were dissected, fixed in paraformaldehyde (PFA), and immunostains of whole mount lungs performed as described (Metzger et al., 2008) except as noted (Supplemental Experimental Procedures), then imaged by confocal microscopy or optical projection tomography. For cryosections, tissue was fixed in PFA or Zamboni's fixative, cryoprotected in 30% sucrose, frozen in OCT, and stored at −80°C. Frozen tissue blocks were sectioned and incubated sequentially with blocking solution, primary antibody, secondary antibody conjugated to Alexa fluorophores, and DAPI. For full description of antibodies and methods, see Supplemental Experimental Procedures.

Mapping pulmonary NE cells

Serial sections of entire left lobes (n=5) of E16 CD-1 mice were stained for E-cadherin and Ascl1, and branches L.L1, L.L2, L.L3, L.L4, L.D1, L.D2, L.D3, L.D4 systematically examined for NE cells. Additional ages and branch points in left and right lung lobes were analyzed as described (Supplemental Experimental Procedures).

Developmental analysis of NE cells

Serial sections of entire left lung lobes (n=5 for each stage examined) of E12-E16 CD-1 mice were stained for Ascl1 and E-cadherin, and positions of NE cells determined in branches and at junctions indicated. For NE cell counts (Fig. S3D), serial sections of the entire left lobe were immunostained for Ascl1 and E-cadherin, and cells scored in each segment along left main bronchus as indicated.

For EdU incorporation, 300 ug EdU was injected intraperitoneally and lungs harvested two hours later. EdU was detected by click chemistry in cryosections immunostained for Ascl1 and counterstained with DAPI, then visualized by confocal microscopy. For phospho-histone H3 analysis, cryosections were immunostained for Ascl1 and anti-phospho-Histone 3-Ser10.

Lineage tracing and clonal analysis

Lineage tracing was done with *Shh* $^{Cre/+}$;*Rosa26* $^{mTmG/+}$ mice (airway epithelial lineage) and with *Wnt1-Cre;Rosa26* $^{Zsgreen/+}$ (neural crest lineage). Lungs were harvested between E17.5-E18.5, fixed, cryosectioned, and immunostained as above. To test monoclonality of NEBs (Fig. 3A), cryosectioned E18 *Shh*$^{Cre/+}$;*Rosa26*$^{Rbw/+}$ lungs, in which all airway epithelial cells are permanently labeled early in development with one of the three Rainbow fluorescent reporters, were immunostained with anti-CGRP and an Alexa633-conjugated secondary. Cell number and colors in each NE cluster were assessed by confocal fluorescence microscopy. For clonal analysis, individual NE progenitors were sparsely labeled by tamoxifen injection at E11.5 (4 mg tamoxifen) or E12.5 (3 or 4 mg) of *Ascl1*$^{CreER/+}$;*Rosa26*$^{Rbw/+}$ mice, and lungs were harvested between E17.5 – E18.5 and analyzed as above.

Labeling NE developmental intermediates

Ascl1$^{CreER/+}$;*Rosa26*$^{ZsGreen/+}$ mice were induced with tamoxifen at E12.5, and lungs were harvested at E14.5 or E15.5 and serially sectioned, then co-stained for PGP9.5, E-cadherin and, for some samples, laminin gamma1 (γ1). NEBs and mini-clusters were analyzed by confocal microscopy, and a 35 – 40 μm z-stack was collected and each labeled NE progenitor examined at high resolution. 3D reconstructions (Volocity) of each progenitor was used to identify cell shape, cytoplasmic processes, and interactions with other cells and basement membrane. Detailed descriptions of the morphologic classes are given in Supplemental Experimental Procedures.

Live imaging of NE cells in slice culture

Ascl1$^{CreER/+}$;*Rosa26*$^{ZsGreen/mTmG}$ mice were induced with tamoxifen by oral gavage at E13 to label pulmonary NE progenitors with ZsGreen and mGFP, and all other cells with TdTomato. At E15, lungs were harvested and left lobes and right caudal lobes separated, embedded in agarose and sectioned (Compresstome). Individual slices (175 μm thick) were transferred to a coverglass chamber, covered with Matrigel, and cultured in DMEM +F12 medium with 10% fetal bovine serum in an environmental chamber at 37°C and 5% CO_2. After 2-3 hours to establish the culture, confocal images were collected every 20 minutes for 60 hours. See Supplemental Experimental Procedures.

Supplementary Material

Refer to Web version on PubMed Central for supplementary material.

Acknowledgements

We thank Makenna Morck for help with slice culture experiments, Jozeph Pendleton for help with mouse colony maintenance, Dr. Andrew Olson (Stanford Neuroscience Microscopy Service, NIH NS069375) for advice on video processing, Dr. Jane Johnson for *Ascl1*^{CreER}, members of the Krasnow lab for discussions and comments on the manuscript, and Maria Petersen for help preparing the manuscript and figures. This work was supported by a grant from the NHLBI Progenitor Cell Biology Consortium, and a Parker B. Francis Foundation Fellowship and NIH NHLBI K12 fellowship (C.K.). MA.K. is an investigator of the Howard Hughes Medical Institute.

References

Aguayo SM, Miller YE, Waldron JAJ, Bogin RM, Sunday ME, Staton GWJ, Beam WR, King TEJ. Brief report: idiopathic diffuse hyperplasia of pulmonary neuroendocrine cells and airways disease. N Engl J Med. 1992; 327:1285–1288. [PubMed: 1406819]

Aigouy B, Farhadifar R, Staple DB, Sagner A, Röper J-C, Julicher F, Eaton S. Cell Flow Reorients the Axis of Planar Polarity in theWing Epithelium of Drosophila. Cell. 2010; 142:773–786. [PubMed: 20813263]

Anderson DJ, Axel R. A bipotential neuroendocrine precursor whose choice of cell fate is determined by NGF and glucocorticoids. Cell. 1986; 47:1079–1090. [PubMed: 2877748]

Batlle E, Henderson JT, Beghtel H, van den Born MMW, Sancho E, Huls G, Meeldijk J, Robertson J, van de Wetering M, Pawson T, et al. Beta-catenin and TCF mediate cell positioning in the intestinal epithelium by controlling the expression of EphB/ephrinB. Cell. 2002; 111:251–263. [PubMed: 12408869]

Bertet C, Sulak L, Lecuit T. Myosin-dependent junction remodeling controls planar cell intercalation and axis elongation. Nature. 2004; 429:667–671. [PubMed: 15190355]

Blankenship JT, Backovic ST, Sanny JSP, Weitz O, Zallen JA. Multicellular rosette formation links planar cell polarity to tissue morphogenesis. Developmental Cell. 2006; 11:459–470. [PubMed: 17011486]

Brouns I, Oztay F, Pintelon I, Proost I, Lembrechts R, Timmermans J-P, Adriaensen D. Neurochemical pattern of the complex innervation of neuroepithelial bodies in mouse lungs. Histochem Cell Biol. 2008; 131:55–74. [PubMed: 18762965]

Chai Y, Jiang X, Ito Y, Bringas PJ, Han J, Rowitch DH, Soriano P, McMahon AP, Sucov HM. Fate of the mammalian cranial neural crest during tooth and mandibular morphogenesis. Development. 2000; 127:1671–1679. [PubMed: 10725243]

Cubas P, de Celis JF, Campuzano S, Modolell J. Proneural clusters of achaete scute expression and the generation of sensory organs in the Drosophila imaginal wing disc. Genes & Development. 1991; 107:996–1008. [PubMed: 2044965]

Cutz E, Perrin DG, Pan J, Haas EA, Krous HF. Pulmonary neuroendocrine cells and neuroepithelial bodies in sudden infant death syndrome: potential markers of airway chemoreceptor dysfunction. Pediatric and Developmental Pathology. 2007; 10:106–116. [PubMed: 17378691]

Cutz E, Pan J, Yeger H, Domnik NJ, Fisher JT. Seminars in Cell & Developmental Biology. Seminars in Cell and Developmental Biology. 2013; 24:40–50. [PubMed: 23022441]

Deterding RR, Pye C, Fan LL, Langston C. Persistent tachypnea of infancy is associated with neuroendocrine cell hyperplasia. Pediatr. Pulmonol. 2005; 40:157–165. [PubMed: 15965897]

Ewald AJ, Brenot A, Duong M, Chan BS, Werb Z. Collective Epithelial Migration and Cell Rearrangements Drive Mammary Branching Morphogenesis. Developmental Cell. 2008; 14:570–581. [PubMed: 18410732]

Feyrter F. [Argyrophilia of bright cell system in bronchial tree in man]. Z Mikrosk Anat Forsch. 1954; 61:73–81. [PubMed: 14374964]

Gillan JE, Cutz E. Abnormal pulmonary bombesin immunoreactive cells in Wilson-Mikity syndrome (pulmonary dysmaturity) and bronchopulmonary dysplasia. Pediatr Pathol. 1993; 13:165–180. [PubMed: 8464778]

Gu G, Dubauskaite J, Melton DA. Direct evidence for the pancreatic lineage: NGN3+ cells are islet progenitors and are distinct from duct progenitors. Development. 2002; 129:2447–2457. [PubMed: 11973276]

Guha A, Vasconcelos M, Cai Y, Yoneda M, Hinds A, Qian J, Li G, Dickel L, Johnson JE, Kimura S, et al. Neuroepithelial body microenvironment is a niche for a distinct subset of Clara-like precursors in the developing airways. Proceedings of the National Academy of Sciences. 2012; 109:12592–12597.

Guillot C, Lecuit T. Mechanics of epithelial tissue homeostasis and morphogenesis. Science. 2013; 340:1185–1189. [PubMed: 23744939]

Harris KS, Zhang Z, McManus MT, Harfe BD, Sun X. Dicer function is essential for lung epithelium morphogenesis. Proc. Natl. Acad. Sci. U.S.a. 2006; 103:2208–2213. [PubMed: 16452165]

Irvine KD, Wieschaus E. Cell intercalation during Drosophila germband extension and its regulation by pair-rule segmentation genes. Development. 1994; 120:827–841. [PubMed: 7600960]

Ito T, Udaka N, Yazawa T, Okudela K, Hayashi H, Sudo T, Guillemot F, Kageyama R, Kitamura H. Basic helix-loop-helix transcription factors regulate the neuroendocrine differentiation of fetal mouse pulmonary epithelium. Development. 2000; 127:3913–3921. [PubMed: 10952889]

Kim EJ, Ables JL, Dickel LK, Eisch AJ, Johnson JE. Ascl1 (Mash1) defines cells with long-term neurogenic potential in subgranular and subventricular zones in adult mouse brain. PLoS ONE. 2011; 6:e18472. [PubMed: 21483754]

Krens SFG, Heisenberg C-P. Cell sorting in development. Curr Top Dev Biol. 2011; 95:189–213. [PubMed: 21501752]

Lamouille S, Xu J, Derynck R. Molecular mechanisms of epithelial-mesenchymal transition. Nat Rev Mol Cell Biol. 2014; 15:178–196. [PubMed: 24556840]

Lauweryns JM, Peuskens JC. Neuro-epithelial bodies (neuroreceptor or secretory organs?) in human infant bronchial and bronchiolar epithelium. Anat. Rec. 1972; 172:471–481. [PubMed: 4110997]

Lauweryns JM, Van Lommel A. Ultrastructure of nerve endings and synaptic junctions in rabbit intrapulmonary neuroepithelial bodies: a single and serial section analysis. Journal of Anatomy. 1987; 151:65–83. [PubMed: 3654362]

Lawrence PA. Development and determination of hairs and bristles in the milkweed bug, Oncopeltus fasciatus (Lygaeidae, Hemiptera). Journal of Cell Science. 1966; 1:475–498. [PubMed: 5956722]

Mani SA, Guo W, Liao M-J, Eaton EN, Ayyanan A, Zhou AY, Brooks M, Reinhard F, Zhang CC, Shipitsin M, et al. The epithelial-mesenchymal transition generates cells with properties of stem cells. Cell. 2008; 133:704–715. [PubMed: 18485877]

Metzger RJ, Klein OD, Martin GR, Krasnow MA. The branching programme of mouse lung development. Nature. 2008; 453:745–750. [PubMed: 18463632]

Morimoto M, Nishinakamura R, Saga Y, Kopan R. Different assemblies of Notch receptors coordinate the distribution of the major bronchial Clara, ciliated and neuroendocrine cells. Development. 2012; 139:4365–4373. [PubMed: 23132245]

Morrison KM, Miesegaes GR, Lumpkin EA, Maricich SM. Developmental Biology. Developmental Biology. 2009; 336:76–83. [PubMed: 19782676]

Nassar AA, Jaroszewski DE, Helmers RA, Colby TV, Patel BM, Mookadam F. Diffuse idiopathic pulmonary neuroendocrine cell hyperplasia: A systematic overview. American Journal of Respiratory and Critical Care Medicine. 2011; 184:8–16. [PubMed: 21471097]

Okubo T, Clark C, Hogan BLM. Cell lineage mapping of taste bud cells and keratinocytes in the mouse tongue and soft palate. Stem Cells. 2009; 27:442–450. [PubMed: 19038788]

Packard A, Georgas K, Michos O, Riccio P, Cebrian C, Combes AN, Ju A, Ferrer- Vaquer A, Hadjantonakis A-K, Zong H, et al. Luminal mitosis drives epithelial cell dispersal within the branching ureteric bud. Developmental Cell. 2013; 27:319–330. [PubMed: 24183650]

Park K-S, Liang M-C, Raiser DM, Zamponi R, Roach RR, Curtis SJ, Walton Z, Schaffer BE, Roake CM, Zmoos A-F, et al. Characterization of the cell of origin for small cell lung cancer. Cell Cycle. 2011; 10:2806–2815. [PubMed: 21822053]

Polak JM, Becker KL, Cutz E, Gail DB, Goniakowska-Witalinska L, Gosney JR, Lauweryns JM, Linnoila I, McDowell EM, Miller YE. Lung endocrine cell markers, peptides, and amines. Anat. Rec. 1993; 236:169–171. [PubMed: 8507003]

Reynolds SD, Hong KU, Giangreco A, Mango GW, Guron C, Morimoto Y, Stripp BR. Conditional clara cell ablation reveals a self-renewing progenitor function of pulmonary neuroendocrine cells. Am. J. Physiol. Lung Cell Mol. Physiol. 2000; 278:L1256–L1263. [PubMed: 10835332]

Rinkevich Y, Lindau P, Ueno H, Longaker MT, Weissman IL. Germ-layer and lineage-restricted stem/progenitors regenerate the mouse digit tip. Nature. 2011; 476:409–413. [PubMed: 21866153]

Rock JR, Hogan BLM. Epithelial progenitor cells in lung development, maintenance, repair, and disease. Annu Rev Cell Dev Biol. 2011; 27:493–512. [PubMed: 21639799]

Scheel C, Weinberg RA. Cancer stem cells and epithelial-mesenchymal transition: concepts and molecular links. Semin Cancer Biol. 2012; 22:396–403. [PubMed: 22554795]

Scheuermann DW. Morphology and cytochemistry of the endocrine epithelial system in the lung. Int Rev Cytol. 1987; 106:35–88. [PubMed: 3294719]

Song H, Yao E, Lin C, Gacayan R, Chen M-H, Chuang P-T. Functional characterization of pulmonary neuroendocrine cells in lung development, injury, and tumorigenesis. Proceedings of the National Academy of Sciences. 2012; 109:17531–17536.

Steinberg MS. Reconstruction of tissues by dissociated cells. Some morphogenetic tissue movements and the sorting out of embryonic cells may have a common explanation. Science. 1963; 141:401–408. [PubMed: 13983728]

Strobl-Mazzulla PH, Bronner ME. Epithelial to mesenchymal transition: new and old insights from the classical neural crest model. Semin Cancer Biol. 2012; 22:411–416. [PubMed: 22575214]

Sutherland KD, Proost N, Brouns I, Adriaensen D, Song J-Y, Berns A. Cell of origin of small cell lung cancer: Inactivation of Trp53 and Rb1 in distinct cell types of adult mouse lung. Cancer Cell. 2011; 19:754–764. [PubMed: 21665149]

Tsao P-N, Vasconcelos M, Izvolsky KI, Qian J, Lu J, Cardoso WV. Notch signaling controls the balance of ciliated and secretory cell fates in developing airways. Development. 2009; 136:2297–2307. [PubMed: 19502490]

Van Keymeulen A, Mascre G, Youseff KK, Harel I, Michaux C, De Geest N, Szpalski C, Achouri Y, Bloch W, Hassan BA, et al. Epidermal progenitors give rise to Merkel cells during embryonic development and adult homeostasis. The Journal of Cell Biology. 2009; 187:91–100. [PubMed: 19786578]

van Meerbeeck JP, Fennell DA, De Ruysscher DKM. Small-cell lung cancer. The Lancet. 2011; 378:1741–1755.

Wright MC, Reed-Geaghan EG, Bolock AM, Fujiyama T, Hoshino M, Maricich SM. Unipotent, Atoh1+ progenitors maintain the Merkel cell population in embryonic and adult mice. The Journal of Cell Biology. 2015; 208:367–379. [PubMed: 25624394]

Young LR, Brody AS, Inge TH, Acton JD, Bokulic RE, Langston C, Deutsch GH. Neuroendocrine cell distribution and frequency distinguish neuroendocrine cell hyperplasia of infancy from other pulmonary disorders. Chest. 2011; 139:1060–1071. [PubMed: 20884725]

Zaccone G, Tagliafierro G, Goniakowska-Witalinska L, Fasulo S, Ainis L, Mauceri A. Serotonin-like immunoreactive cells in the pulmonary epithelium of ancient fish species. Histochemistry. 1989; 92:61–63. [PubMed: 2570048]

Highlights

- Neuroendocrine cells form clusters at stereotyped positions at branch junctions
- Progenitors are selected randomly in epithelium but rapidly sort from other cells
- Sorting occurs by directed migration of progenitors to branch junctions
- Migrating cells undergo transient EMT, crawling over neighbor cells to the target

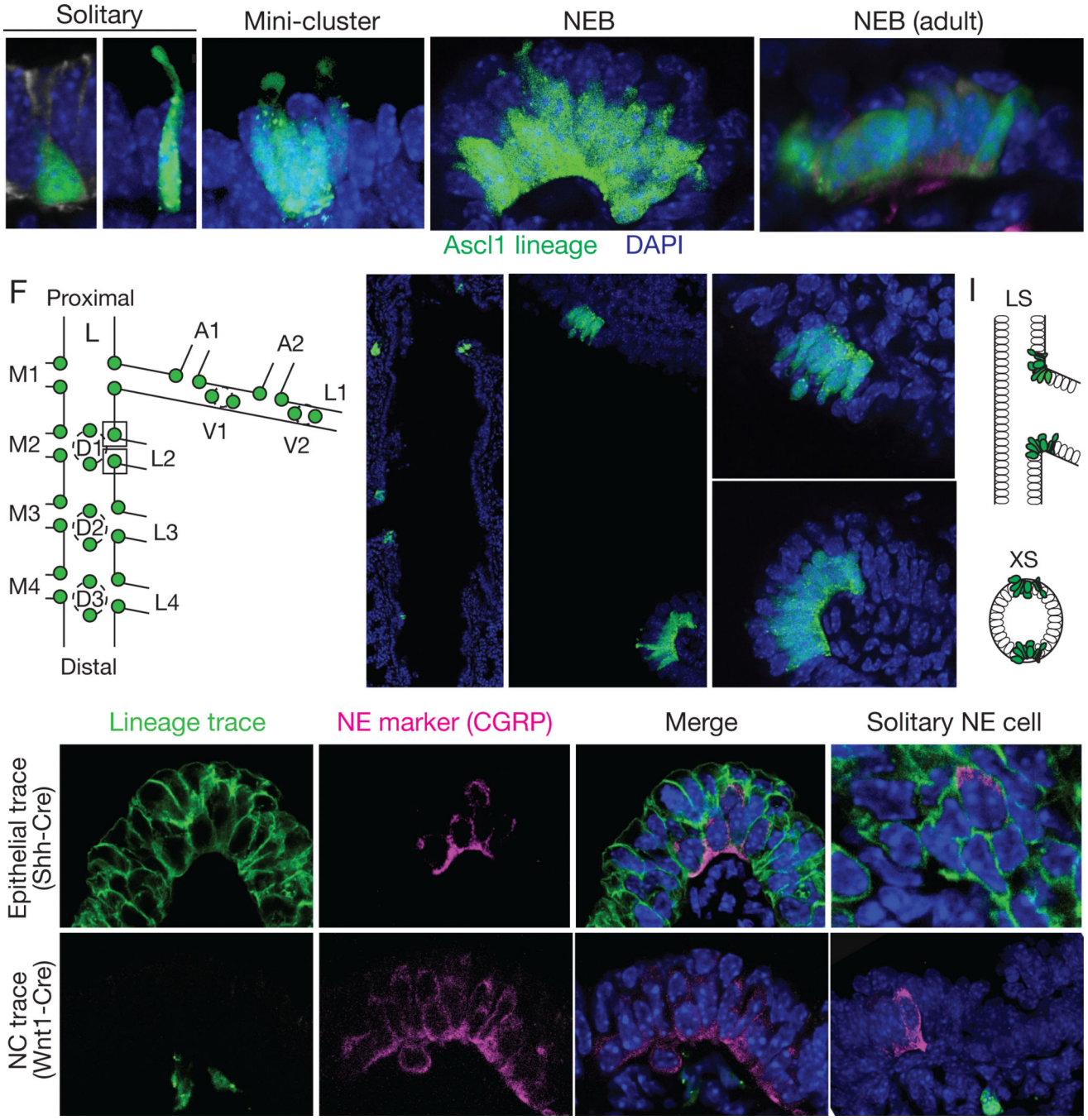

Figure 1. Mapping and lineage tracing of pulmonary neuroendocrine cells

(A-E) Confocal images of NE cells in bronchial epithelium of embryonic day (E) 18 (A-D) or adult (postnatal 2 month; E) *Ascl1*$^{CreER/+}$;*Rosa26*$^{ZsGreen/+}$mouse induced with tamoxifen at E14 to label NE cells with ZsGreen (green). See also Figure S1. (A,B) Solitary NE cells with pyramidal (A) and slender (B) morphologies. Arrowhead, thin projection to lumen. (C) Mini-cluster of 4 NE cells. (D) Neuroepithelial body (NEB), a large cluster of ~25 NE cells (12 visible in optical plane). (E) Adult NEB. Cells are more uniformly columnar. Note non-NE cells (nuclei marked by dots) superficial to NE cells in NEBs (D,E). Sample was also

stained with PGP9.5 (red) to confirm NE identity and show innervating fibers (arrowhead). Dotted lines, individual NE cells in clusters; dashed lines, basement membrane location determined by co-staining with E-cadherin or laminin γ1. Bar, 10 μm.

(F-I) Stereotyped locations of NEBs at airway branchpoints. (F) Left primary bronchus (L) and some daughter (L.L1, L.L2, ...) and granddaughter (L.L1.A1, L.L1.A2,...) branches showing positions of NEBs at E18. (G) Low magnification confocal image of left primary bronchus of E18 *Ascl1*$^{CreER/+}$;*Rosa26*$^{ZsGreen/+}$ mouse. Note pairs of NEBs (green) at indicated branch points (L.L2, L.M3), with one NEB located proximal (p) and the other distal (d) along bronchial tree. (H) Longitudinal optical section through base of L.L2 showing L.L2p and L.L2d NEBs. Closeups of NEBs (boxed) are shown at right. Bar, 5 μm. (I) Schematic longitudinal section (LS) and cross section (XS) showing diametrically-opposite positions of L.L2 NEBs at branch base. (See also Figure S2).

(J-M) Lineage tracing of NE cell origins. Confocal images of NEBs (J,L) and solitary NE cells (K,M) at E18 from *Shh*$^{Cre/+}$;*Rosa26*$^{mTmG/+}$ mouse to label bronchial epithelial lineage (J,K) or from *Wnt1-Cre;Rosa26*$^{ZsGreen/+}$ mouse to label neural crest lineage (L,M). Lungs were co-stained for lineage tag (green) and NE marker CGRP (magenta). All NEB and solitary NE cells express bronchial trace and none express neural crest trace. Other epithelial cells also express bronchial trace, and sub-epithelial neurons (arrowheads) express Wnt1 trace. Dots, outline of NEBs or individual NE cells; dashes, basement membrane. Bar, 10 μm.

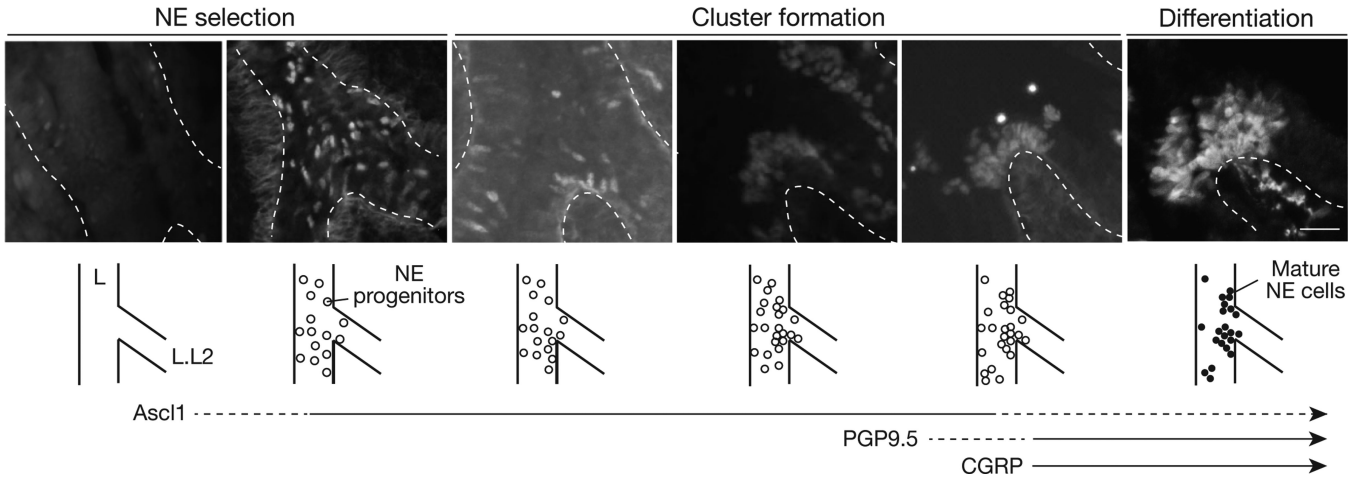

Figure 2. Cellular events in NEB formation

Longitudinal optical sections and schematics of base of L.L2 bronchus at stages indicated in wild type lungs stained for NE progenitor marker Ascl1 (A-E) or mature marker PGP9.5 (F). Dashed lines, basement membrane. Three phases of NEB development are indicated: NE cell selection in bronchial epithelium, as indicated by expression of Ascl1 (open circles); NE cell cluster formation at NEB sites; and differentiation marked by expression of PGP9.5 (filled circles) and CGRP (see Figure S3F). Timing of Ascl1, PGP9.5, and CGRP expression is indicated below. PGP9.5-positive nerve fibers (arrowhead, F) extend toward and begin to ramify on L.L2 NEB at E16.5. Bar, 25 μm. See also Figure S3.

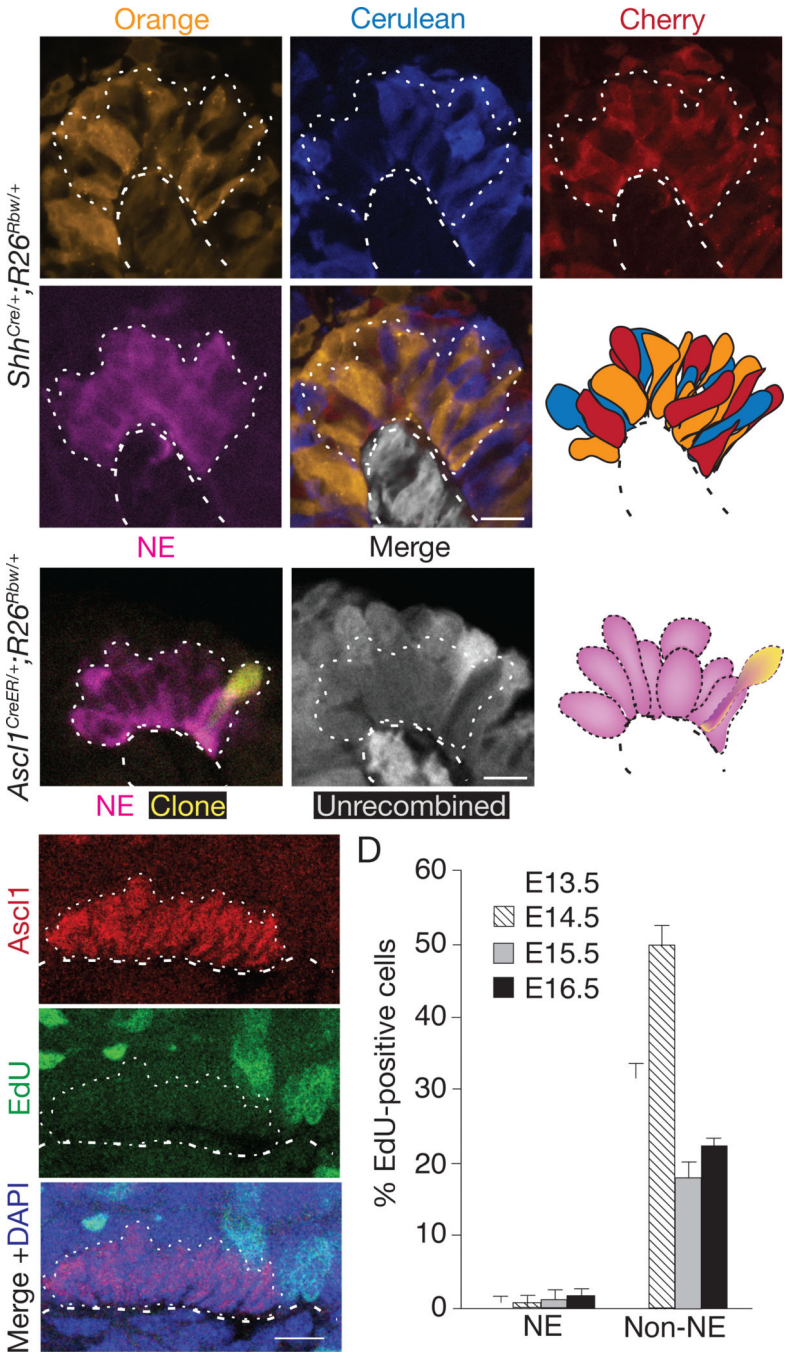

Figure 3. Analysis of proliferation during NEB formation

(A) Close-up of NEB in *Shh*$^{Cre/+}$;*Rosa26*$^{Rbw/+}$ mouse lung in which entire bronchial epithelium was permanently labeled with one of the Rainbow reporters (Orange, Cerulean, or Cherry) before NE selection then co-stained for CGRP (magenta) at E18 following NEB formation. NEB (dotted outline) is composed of cells labeled with each of the reporters, thus it did not arise by proliferation of a single progenitor. Epithelial cells neighboring the NEB are not shown in schematic; cells below basement membrane (dashed line) express the

constitutive (expressed in absence of Cre) GFP reporter (pseudo-colored gray). Bar, 10 μm. See also Table S1.

(B) Close-up of a NEB in E18 *Ascl1*$^{CreER/+}$;*Rosa26*$^{Rbw/+}$ mouse lung in which NE progenitors were sparsely labeled by injection of tamoxifen (4 mg) early in NE development (E11.5) then immunostained for CGRP (magenta) six days later following NEB formation. Note one labeled cell (pseudocolored yellow) in NEB, indicating that labeled progenitor did not proliferate. Cells without Cre activity ("Unrecombined") express the GFP reporter (pseudo-colored gray in middle panel); note absence of GFP in clone (Orange-expressing cell). Only cells in NEB (dotted lines) are shown in schematic. Bar, 10 μm. See also Tables S2A-C.

(C) Confocal sagittal section through cluster of NE cells during NEB formation in E14 wild type embryo in which EdU was injected two hours before harvesting to label dividing cells, then analyzed after co-staining for EdU (green) and Ascl1 (red). No NE cells, but many surrounding epithelial cells, are labeled with EdU. (D) Quantification of EdU-positive NE and non-NE airway epithelial cells at indicated ages. Values shown are percent +/−S.E. for proportions (n=134, 119, 78, 130 (NE cells), n=520, 322, 326, 930 (non-NE cells) at E13.5, 14.5, 15.5, 16.5, respectively) scored in 2 embryos for each cell type scored at each age. Note few EdU-positive NE cells, indicating progenitors exit cell cycle at or just after selection. Similar results were obtained for phospho-histone H3 analysis. Bar, 10 μm.

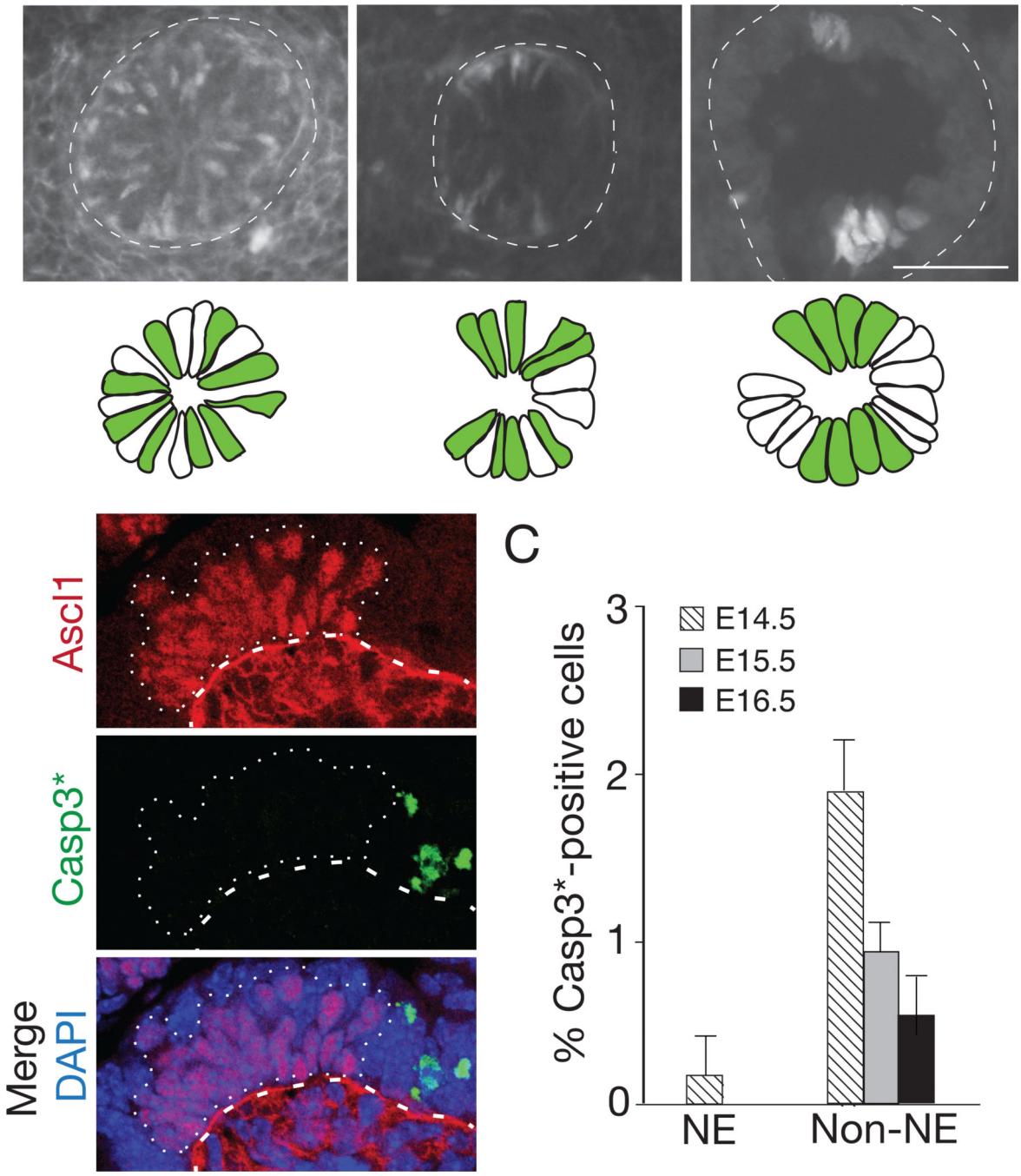

Figure 4. Local clearing of NE cell precursors during cluster formation

(A) Cross-sections through base of bronchial branch L.V2 at indicated ages of wild type embryos immunostained for Ascl1 (white; green in schematics below) to show NE progenitors forming NEBs L.V2p and L.V2d. Progenitors are initially scattered in “salt and pepper” pattern but, as NEBs form, surrounding regions clear of NE cells. Bar, 10 μm. (B) Sagittal section through developing NEB (dotted outline) in E14 lung co-stained for Ascl1 (red) and activated (cleaved) Caspase 3 (Casp3*, green) to detect apoptotic cells. Note Casp3*-positive cells near, but not within, NEB (dotted outline). Ascl1 signal below

basement membrane (dashed line) at E13 is non-specific background. Bar, 10 μm. (C) Quantification of Casp3*-positive NE and non-NE cells in bronchial epithelium at indicated stages. Data shown are percent ± S.E. for proportions; n=589, 406, 322 (NE cells), 1437, 1534, 1122 (non-NE cells) scored at E14.5, 15.5, 16.5, respectively, from 2 embryos at each stage.

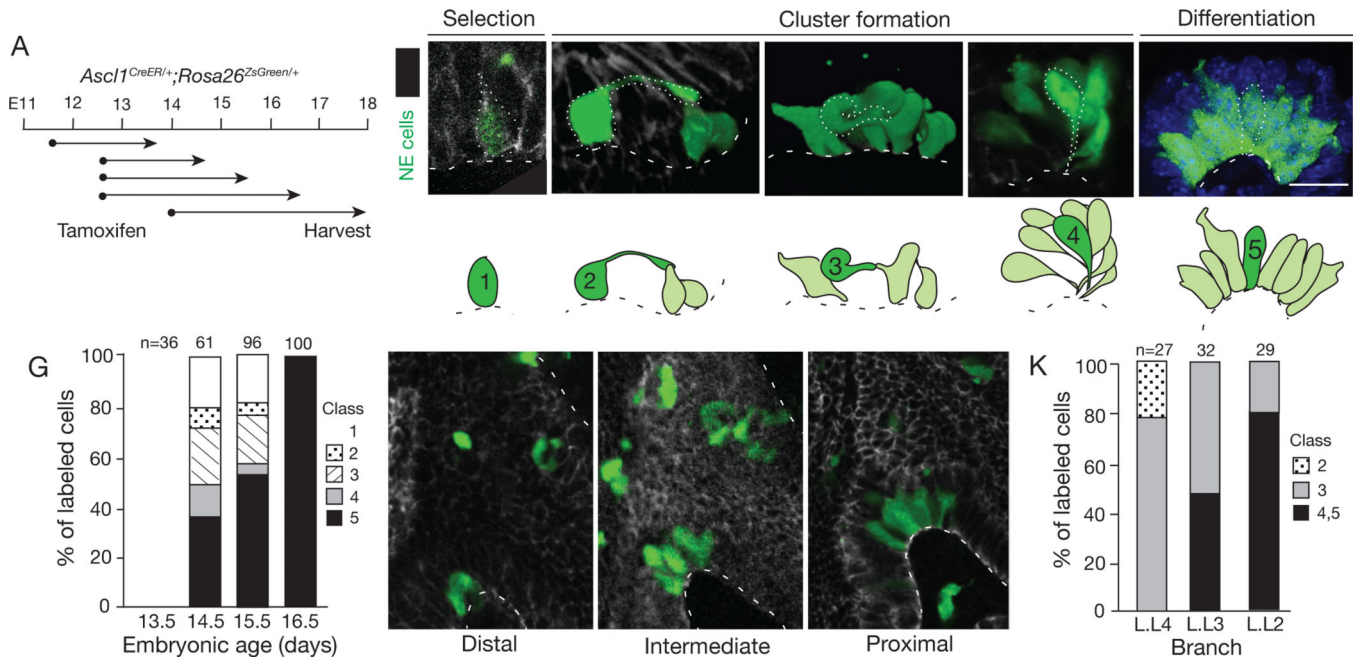

Figure 5. Sparse labeling of progenitors reveals a series of NEB intermediates

(A) Labeling scheme. NE progenitors were permanently labeled with ZsGreen by tamoxifen injection of *Ascl1*$^{CreER/+}$;*Rosa26*$^{ZsGreen/+}$ mice at indicated ages (dots), then allowed to develop for times indicated (arrows).

(B-F) Micrographs and schematics of five classes of NE intermediates (green) labeled as above and co-stained for E-cadherin to outline epithelial cells. A representative cell of each class is outlined (dots) in micrograph and highlighted in dark green in schematic; other labeled NE cells are shown in light green in schematic. Note long (>10 μm) apical cell extension (class 2), fibroblast-like morphology and no basement membrane contact (class 3), and thin cellular extensions that converge at basement membrane (class 4). In late embryo (~E17) through adult, all NE cells contact basement membrane (class 5). Bar, 10 μm. See also Figures S5A,B and Table S3.

(G) Quantification of different classes of NEB intermediates labeled as above and harvested 48 hours after tamoxifen injection at ages indicated. The changing abundance of intermediates supports their ordering in a developmental series. n, number of intermediates scored in 2 lungs at each stage.

(H-K) Confocal images (sagittal sections; H-J) and quantification (K) of NEB intermediates labeled as above at base of bronchi L.L4, L.L3, and L.L2 in same lung. L.L4 is most distal (immature) and L.L2 is most proximal (mature) position. The different abundance of intermediates along proximal-distal axis supports their ordering in a developmental series. n, number of intermediates scored in 2 embryos. Bar, 10 μm.

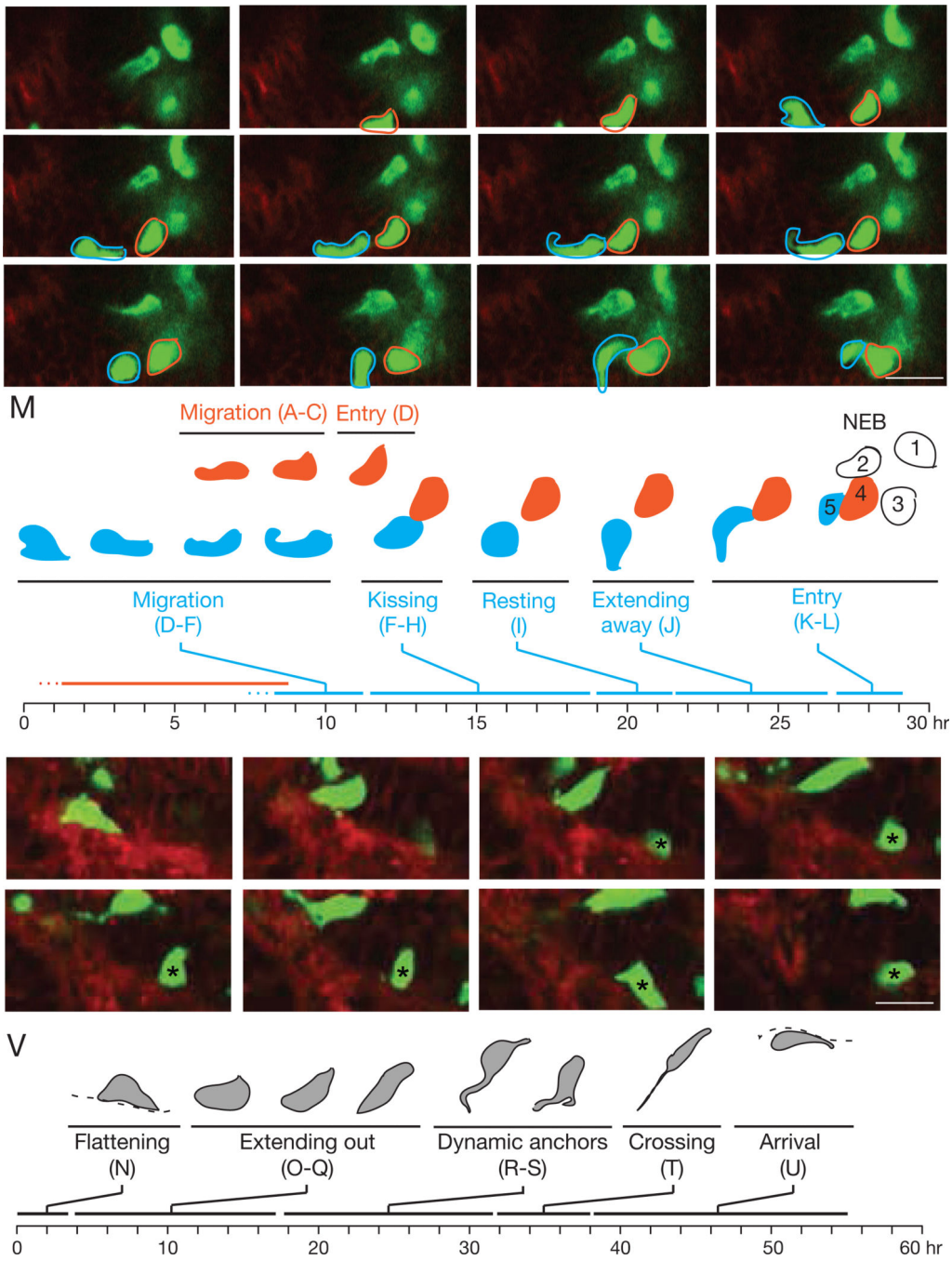

Figure 6. Live imaging of migrating NE progenitors in lung slice culture

(A-L) NE cell migration and entry into NEB. Selected frames from 26 hour time-lapse confocal microscopy (Movie S1) of migrating NE cells in E15 mouse lung slice culture from *Asc1*$^{CreER/+}$;*Rosa26*$^{ZsGreen/mTmG}$ mouse induced with tamoxifen at E13 to label NE cells with ZsGreen and mGFP (green) and other cells with mTomato (red). NE cells 1-3 at developing NEB site are joined by cell 4 (red outline), which migrates into region (B, C; at ~1.6 μm/hr) and directly enters cluster (D). Cell 5 (blue outline) migrates into same region (D; ~1.6 μm/hr) but soon changes direction and extends toward cell 4 (E). Cell 4

reciprocates (F) and the cells contact briefly (G, “kissing”) and retract (H), repeating kissing sequence 4 times in ~5 hours. Over the next 5 hours, cell 5 remains stationary (I, “resting”) before extending backward (J, “extending away”) and then diving forward (K, “entry”) to join NEB cluster (L).

(M) Timeline of above changes in cell 4 (red) and 5 (blue).

(N-U) NE cell crossing bronchial tube. Selected frames from another region of same culture. Initially, NE cell flattens along basement membrane (N, “flattening”) then re-orients toward lumen (O-Q, “extending out”). Over next ~14 hours, its contact with basement changes dynamically (R,S, “dynamic anchors”), including formation of a second extension that contacts basement membrane >10 μm away (S). Just before crossing, anchor is a very fine projection with “beaded” appearance (T) that fragments as cell finally crosses (~2.5 μm/hr) into epithelium of opposing side of tube (crossing, T) to reach destination (U, arrival). Frame U was selected from a z-plane 8 μm deeper than panels N-T to more clearly visualize cell after arrival. Dashed line, basement membrane. Bar, 10 μm. See also Movies S1, S2.

(V) Timeline of above changes.

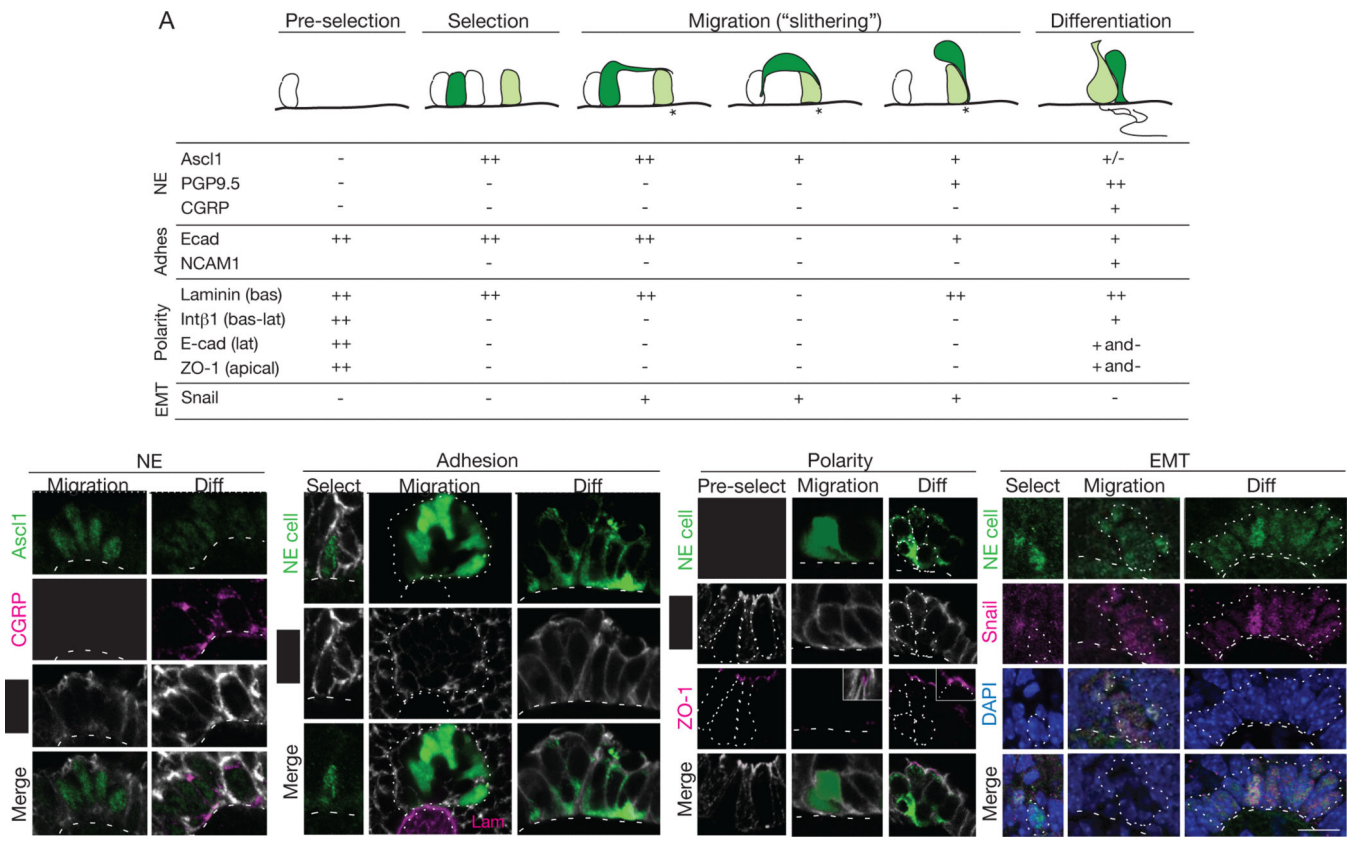

Figure 7. NE progenitors transiently express EMT regulator Snail and downregulate adhesion and polarity markers

(A) Expression of NE, adhesion (adhes), polarity, and EMT markers in NEB progenitors and intermediates (dark green) at steps indicated: before NE selection (pre-selection) and during NE specification (Class 1), migration to form clusters (Classes 2-4), and differentiation (Class 5). Light green cells, maturing NE cell already at target (asterisk); white cells, NE cells before selection and other non-NE epithelial cells. Symbols show high (++), intermediate (+), low (+/−), no (−), or mixed (+ and −) expression. For polarity markers, expression refers to expression restricted to basal (bas), basolateral (bas-lat), or apical domains. See also Figure S7.

(B-E) Confocal micrographs showing dynamic patterns of indicated NE (B), adhesion (C), polarity (D) and EMT (E) markers at indicated steps of NEB formation. Dots, outline of NEB; dashed line, basement membrane. (B) Ascl1 (green) is expressed during migration (left panels; E13) but down-regulated during differentiation (right panels; E18), whereas CGRP (red) is detected only during differentiation. (C) E-cadherin is expressed around entire plasma membrane during NE selection (Ascl1-positive (green) cell at E13; left panels), but is down-regulated in class 3 and 4 intermediates (some of which are marked by ZsGreen in E15 *Ascl1*$^{CreER/+}$;*Rosa26*$^{ZsGreen/+}$ mouse induced with tamoxifen at E12.5) in developing NEB (dotted outline; center panels). E-cadherin is again detected in NE cells (CGRP-positive; green) of mature NEB (PN 2 month; right panels), although expression is excluded from apical cell surface and detected along lateral boundaries in at least some cells. Cells neighboring NEB (not shown) express higher levels of E-cadherin and have larger

apical surface that excludes E-cadherin. (D) Before NE selection (E12; left panels) epithelial progenitors are uniformly polarized and tight junction protein ZO-1 (magenta) is detected at apical surface of each cell. ZO-1 is down-regulated and undetected in intermediates (*Ascl1*$^{CreER/+}$;*Rosa26*$^{ZsGreen/+}$ mouse labeled as above) during migration (center panels),when surrounding epithelial cells maintain its expression (inset), but is again detected during differentiation (right panels). (E) Snail proteins (magenta) are detected in some (filled arrowhead) but not other (open arrowhead) early NE progenitors (Ascl1-positive, green) during NE selection (E13; left panels), but all intermediates express Snail during migration (middle panels). Intermediates down-regulate Snail in concert with Ascl1 as clusters form and differentiate (E15; right panels), as seen by declining level of Snail and Ascl1 in some cells (asterisks) within maturing cluster. Snail proteins are induced again later in NE cells (C.K., Joe Ouadah, and M.A.K., unpublished data). Bars, 10 μm.